



CERN-PPE/92-89

29<sup>th</sup> May 1992.

# A study of two-particle momentum correlations in hadronic $Z^0$ decays

The OPAL Collaboration

## Abstract

We report on a measurement of two-particle momentum correlations in hadronic decays of the  $Z^0$  at LEP. These data are compared with recent analytic QCD calculations based on the summation of leading and next-to-leading logarithms, and with QCD Monte Carlo simulations. We find that the analytic calculations show the same general features as the data, but that the overall level of the correlations is not reproduced, suggesting that higher order or hadronization effects are significant. This contrasts with the success of similar QCD calculations in describing single-particle momentum distributions. QCD Monte Carlo models are found to give a reasonable level of correlation, with parton shower models incorporating string hadronization giving the best description of the data.

(Submitted to Physics Letters B )

# The OPAL Collaboration

P.D. Acton<sup>25</sup>, G. Alexander<sup>23</sup>, J. Allison<sup>16</sup>, P.P. Allport<sup>5</sup>, K.J. Anderson<sup>9</sup>, S. Arcelli<sup>2</sup>,  
A. Astbury<sup>28</sup>, D. Axen<sup>29</sup>, G. Azuelos<sup>18,a</sup>, G.A. Bahan<sup>16</sup>, J.T.M. Baines<sup>16</sup>,  
A.H. Ball<sup>17</sup>, J. Banks<sup>16</sup>, G.J. Barker<sup>13</sup>, R.J. Barlow<sup>16</sup>, S. Barnett<sup>16</sup>, J.R. Batley<sup>5</sup>,  
G. Beaudoin<sup>18</sup>, A. Beck<sup>23</sup>, J. Becker<sup>10</sup>, T. Behnke<sup>27</sup>, K.W. Bell<sup>20</sup>, G. Bella<sup>23</sup>,  
P. Berlich<sup>10</sup>, S. Bethke<sup>11</sup>, O. Biebel<sup>3</sup>, U. Binder<sup>10</sup>, I.J. Bloodworth<sup>1</sup>, P. Bock<sup>11</sup>,  
B. Boden<sup>3</sup>, H.M. Bosch<sup>11</sup>, S. Bougerolle<sup>29</sup>, H. Breuker<sup>8</sup>, R.M. Brown<sup>20</sup>, R. Brun<sup>8</sup>,  
A. Buijs<sup>8</sup>, H.J. Burckhart<sup>8</sup>, P. Capiluppi<sup>2</sup>, R.K. Carnegie<sup>6</sup>, A.A. Carter<sup>13</sup>,  
J.R. Carter<sup>5</sup>, C.Y. Chang<sup>17</sup>, D.G. Charlton<sup>8</sup>, P.E.L. Clarke<sup>25</sup>, I. Cohen<sup>23</sup>,  
W.J. Collins<sup>5</sup>, J.E. Conboy<sup>15</sup>, M. Cooper<sup>22</sup>, M. Couch<sup>1</sup>, M. Coupland<sup>14</sup>, M. Cuffiani<sup>2</sup>,  
S. Dado<sup>22</sup>, G.M. Dallavalle<sup>2</sup>, S. De Jong<sup>8</sup>, L.A. del Pozo<sup>5</sup>, M.M. Deninno<sup>2</sup>,  
A. Dieckmann<sup>11</sup>, M. Dittmar<sup>4</sup>, M.S. Dixit<sup>7</sup>, E. do Couto e Silva<sup>12</sup>, J.E. Duboscq<sup>8</sup>,  
E. Duchovni<sup>26</sup>, G. Duckeck<sup>11</sup>, I.P. Duerdoth<sup>16</sup>, D.J.P. Dumas<sup>6</sup>, P.A. Elcombe<sup>5</sup>,  
P.G. Estabrooks<sup>6</sup>, E. Etzion<sup>23</sup>, H.G. Evans<sup>9</sup>, F. Fabbri<sup>2</sup>, M. Fincke-Keeler<sup>28</sup>,  
H.M. Fischer<sup>3</sup>, D.G. Fong<sup>17</sup>, C. Fukunaga<sup>24,b</sup>, A. Gaidot<sup>21</sup>, O. Ganel<sup>26</sup>, J.W. Gary<sup>4</sup>,  
J. Gascon<sup>18</sup>, R.F. McGowan<sup>16</sup>, N.I. Geddes<sup>20</sup>, C. Geich-Gimbel<sup>3</sup>, S.W. Gensler<sup>9</sup>,  
F.X. Gentit<sup>21</sup>, G. Giacomelli<sup>2</sup>, V. Gibson<sup>5</sup>, W.R. Gibson<sup>13</sup>, J.D. Gillies<sup>20</sup>,  
J. Goldberg<sup>22</sup>, M.J. Goodrick<sup>5</sup>, W. Gorn<sup>4</sup>, C. Grandi<sup>2</sup>, F.C. Grant<sup>5</sup>, J. Hagemann<sup>27</sup>,  
G.G. Hanson<sup>12</sup>, M. Hansroul<sup>8</sup>, C.K. Hargrove<sup>7</sup>, P.F. Harrison<sup>13</sup>, J. Hart<sup>8</sup>,  
P.M. Hattersley<sup>1</sup>, M. Hauschild<sup>8</sup>, C.M. Hawkes<sup>8</sup>, E. Heflin<sup>4</sup>, R.J. Hemingway<sup>6</sup>,  
R.D. Heuer<sup>8</sup>, J.C. Hill<sup>5</sup>, S.J. Hillier<sup>1</sup>, D.A. Hinshaw<sup>18</sup>, J.D. Hobbs<sup>8</sup>, P.R. Hobson<sup>25</sup>,  
D. Hochman<sup>26</sup>, R.J. Homer<sup>1</sup>, A.K. Honma<sup>28,a</sup>, S.R. Hou<sup>17</sup>, C.P. Howarth<sup>15</sup>,  
R.E. Hughes-Jones<sup>16</sup>, R. Humbert<sup>10</sup>, P. Igo-Kemenes<sup>11</sup>, H. Ihssen<sup>11</sup>, D.C. Imrie<sup>25</sup>,  
A.C. Janissen<sup>6</sup>, A. Jawahery<sup>17</sup>, P.W. Jeffreys<sup>20</sup>, H. Jeremie<sup>18</sup>, M. Jimack<sup>2</sup>, M. Jobs<sup>1</sup>,  
R.W.L. Jones<sup>13</sup>, P. Jovanovic<sup>1</sup>, D. Karlen<sup>6</sup>, K. Kawagoe<sup>24</sup>, T. Kawamoto<sup>24</sup>,  
R.K. Keeler<sup>28</sup>, R.G. Kellogg<sup>17</sup>, B.W. Kennedy<sup>15</sup>, D.E. Klem<sup>7</sup>, T. Kobayashi<sup>24</sup>,  
T.P. Kokott<sup>3</sup>, S. Komamiya<sup>24</sup>, L. Köpke<sup>8</sup>, J.F. Kral<sup>8</sup>, R. Kowalewski<sup>6</sup>, J. von  
Krogh<sup>11</sup>, J. Kroll<sup>9</sup>, M. Kuwano<sup>24</sup>, P. Kyberd<sup>13</sup>, G.D. Lafferty<sup>16</sup>, F. Lamarche<sup>18</sup>,  
J.G. Layter<sup>4</sup>, P. Le Du<sup>21</sup>, P. Leblanc<sup>18</sup>, A.M. Lee<sup>17</sup>, M.H. Lehto<sup>15</sup>, D. Lellouch<sup>26</sup>,  
P. Lennert<sup>11</sup>, C. Leroy<sup>18</sup>, J. Letts<sup>4</sup>, S. Levegrün<sup>3</sup>, L. Levinson<sup>26</sup>, S.L. Lloyd<sup>13</sup>,  
F.K. Loebinger<sup>16</sup>, J.M. Lorah<sup>17</sup>, B. Lorazo<sup>18</sup>, M.J. Losty<sup>7</sup>, X.C. Lou<sup>12</sup>, J. Ludwig<sup>10</sup>,  
M. Mannelli<sup>8</sup>, S. Marcellini<sup>2</sup>, G. Maringer<sup>3</sup>, A.J. Martin<sup>13</sup>, J.P. Martin<sup>18</sup>,  
T. Mashimo<sup>24</sup>, P. Mättig<sup>3</sup>, U. Maur<sup>3</sup>, J. McKenna<sup>28</sup>, T.J. McMahon<sup>1</sup>,  
J.R. McNutt<sup>25</sup>, F. Meijers<sup>8</sup>, D. Menszner<sup>11</sup>, F.S. Merritt<sup>9</sup>, H. Mes<sup>7</sup>, A. Michelini<sup>8</sup>,  
R.P. Middleton<sup>20</sup>, G. Mikenberg<sup>26</sup>, J. Mildenberger<sup>6</sup>, D.J. Miller<sup>15</sup>, R. Mir<sup>12</sup>,  
W. Mohr<sup>10</sup>, C. Moisan<sup>18</sup>, A. Montanari<sup>2</sup>, T. Mori<sup>24</sup>, T. Mouthuy<sup>12,c</sup>, B. Nellen<sup>3</sup>,  
H.H. Nguyen<sup>9</sup>, S.W. O'Neale<sup>8,d</sup>, F.G. Oakham<sup>7</sup>, F. Odorici<sup>2</sup>, M. Ogg<sup>6</sup>, H.O. Ogren<sup>12</sup>,  
H. Oh<sup>4</sup>, C.J. Oram<sup>28,a</sup>, M.J. Oreglia<sup>9</sup>, S. Orito<sup>24</sup>, J.P. Pansart<sup>21</sup>, B. Panzer-Steindel<sup>8</sup>,  
P. Paschievici<sup>26</sup>, G.N. Patrick<sup>20</sup>, N. Paz-Jaoshvili<sup>23</sup>, P. Pfister<sup>10</sup>, J.E. Pilcher<sup>9</sup>,  
D. Pitman<sup>28</sup>, D.E. Plane<sup>8</sup>, P. Poffenberger<sup>28</sup>, B. Poli<sup>2</sup>, A. Pouladdej<sup>6</sup>, E. Prebys<sup>8</sup>,  
T.W. Pritchard<sup>13</sup>, H. Przysiezniak<sup>18</sup>, G. Quast<sup>27</sup>, M.W. Redmond<sup>9</sup>, D.L. Rees<sup>1</sup>,  
G.E. Richards<sup>16</sup>, K. Riles<sup>4</sup>, S.A. Robins<sup>13</sup>, D. Robinson<sup>8</sup>, A. Rollnik<sup>3</sup>, J.M. Roney<sup>9</sup>,  
E. Ros<sup>8</sup>, S. Rossberg<sup>10</sup>, A.M. Rossi<sup>2,e</sup>, M. Rosvick<sup>28</sup>, P. Routenburg<sup>6</sup>, K. Runge<sup>10</sup>,  
O. Runolfsson<sup>8</sup>, D.R. Rust<sup>12</sup>, S. Sanghera<sup>6</sup>, M. Sasaki<sup>24</sup>, C. Sbarra<sup>8</sup>, A.D. Schaile<sup>10</sup>,  
O. Schaile<sup>10</sup>, W. Schappert<sup>6</sup>, P. Scharff-Hansen<sup>8</sup>, P. Schenk<sup>28</sup>, H. von der Schmitt<sup>11</sup>,

<sup>25</sup>Brunel University, Uxbridge, Middlesex, UB8 3PH UK

<sup>26</sup>Nuclear Physics Department, Weizmann Institute of Science, Rehovot, 76100, Israel

<sup>27</sup>Universität Hamburg/DESY, II Inst für Experimental Physik, 2000 Hamburg 52, Germany

<sup>28</sup>University of Victoria, Dept of Physics, P O Box 3055, Victoria BC V8W 3P6, Canada

<sup>29</sup>University of British Columbia, Dept of Physics, 6224 Agriculture Road, Vancouver BC V6T 1Z1, Canada

<sup>a</sup>Also at TRIUMF, Vancouver, Canada V6T 2A3

<sup>b</sup>Now at Meiji Gakuin University, Yokohama 244, Japan

<sup>c</sup>Now at Centre de Physique des Particules de Marseille, Faculté des Sciences de Luminy, Marseille

<sup>d</sup>On leave from Birmingham University, Birmingham B15 2TT, UK

<sup>e</sup>Now at Dipartimento di Fisica, Università della Calabria and INFN, 87036 Rende, Italy

<sup>f</sup>And IPP, McGill University, High Energy Physics Department, 3600 University Str, Montreal, Quebec H3A 2T8, Canada

<sup>g</sup>Now at Dept of Physics, University of Oregon, Eugene, Oregon 97405

<sup>h</sup>Also at Shinshu University, Matsumoto 390, Japan

S. Schreiber<sup>3</sup>, C. Schwick<sup>27</sup>, J. Schwiening<sup>3</sup>, W.G. Scott<sup>20</sup>, M. Settles<sup>12</sup>, B.C. Shen<sup>4</sup>,  
P. Sherwood<sup>15</sup>, R. Shypit<sup>29</sup>, A. Simon<sup>3</sup>, P. Singh<sup>13</sup>, G.P. Sirolì<sup>2</sup>, A. Skuja<sup>17</sup>,  
A.M. Smith<sup>8</sup>, T.J. Smith<sup>8</sup>, G.A. Snow<sup>17</sup>, R. Sobie<sup>28,f</sup>, R.W. Springer<sup>17</sup>,  
M. Sproston<sup>20</sup>, K. Stephens<sup>16</sup>, J. Steuerer<sup>28</sup>, R. Ströhmer<sup>11</sup>, D. Strom<sup>9,g</sup>,  
H. Takeda<sup>24</sup>, T. Takeshita<sup>24,h</sup>, P. Taras<sup>18</sup>, S. Tarem<sup>26</sup>, P. Teixeira-Dias<sup>11</sup>, N. Tesch<sup>3</sup>,  
N.J. Thackray<sup>1</sup>, G. Transtomer<sup>25</sup>, N.J. Tresilian<sup>16</sup>, T. Tsukamoto<sup>24</sup>, M.F. Turner<sup>5</sup>,  
G. Tysarczyk-Niemeyer<sup>11</sup>, D. Van den plas<sup>18</sup>, R. Van Kooten<sup>8</sup>, G.J. VanDalen<sup>4</sup>,  
G. Vasseur<sup>21</sup>, C.J. Virtue<sup>7</sup>, A. Wagner<sup>27</sup>, D.L. Wagner<sup>9</sup>, C. Wahl<sup>10</sup>, J.P. Walker<sup>1</sup>,  
C.P. Ward<sup>5</sup>, D.R. Ward<sup>5</sup>, P.M. Watkins<sup>1</sup>, A.T. Watson<sup>1</sup>, N.K. Watson<sup>8</sup>, M. Weber<sup>11</sup>,  
P. Weber<sup>6</sup>, S. Weisz<sup>8</sup>, P.S. Wells<sup>8</sup>, N. Wermes<sup>11</sup>, M.A. Whalley<sup>1</sup>, G.W. Wilson<sup>21</sup>,  
J.A. Wilson<sup>1</sup>, V-H. Winterer<sup>10</sup>, T. Wlodek<sup>26</sup>, S. Wotton<sup>11</sup>, T.R. Wyatt<sup>16</sup>, R. Yaari<sup>26</sup>,  
G. Yekutieli<sup>26</sup>, M. Yurko<sup>18</sup>, W. Zeuner<sup>8</sup>, G.T. Zorn<sup>17</sup>.

<sup>1</sup>School of Physics and Space Research, University of Birmingham, Birmingham, B15 2TT, UK

<sup>2</sup>Dipartimento di Fisica dell' Università di Bologna and INFN, Bologna, 40126, Italy

<sup>3</sup>Physikalisches Institut, Universität Bonn, D-5300 Bonn 1, FRG

<sup>4</sup>Department of Physics, University of California, Riverside, CA 92521 USA

<sup>5</sup>Cavendish Laboratory, Cambridge, CB3 0HE, UK

<sup>6</sup>Carleton University, Dept of Physics, Colonel By Drive, Ottawa, Ontario K1S 5B6, Canada

<sup>7</sup>Centre for Research in Particle Physics, Carleton University, Ottawa, Ontario K1S 5B6, Canada

<sup>8</sup>CERN, European Organisation for Particle Physics, 1211 Geneva 23, Switzerland

<sup>9</sup>Enrico Fermi Institute and Department of Physics, University of Chicago, Chicago Illinois 60637, USA

<sup>10</sup>Fakultät für Physik, Albert Ludwigs Universität, D-7800 Freiburg, FRG

<sup>11</sup>Physikalisches Institut, Universität Heidelberg, Heidelberg, FRG

<sup>12</sup>Indiana University, Dept of Physics, Swain Hall West 117, Bloomington, Indiana 47405, USA

<sup>13</sup>Queen Mary and Westfield College, University of London, London, E1 4NS, UK

<sup>14</sup>Birkbeck College, London, WC1E 7HV, UK

<sup>15</sup>University College London, London, WC1E 6BT, UK

<sup>16</sup>Department of Physics, Schuster Laboratory, The University, Manchester, M13 9PL, UK

<sup>17</sup>Department of Physics and Astronomy, University of Maryland, College Park, Maryland 20742, USA

<sup>18</sup>Laboratoire de Physique Nucléaire, Université de Montréal, Montréal, Quebec, H3C 3J7, Canada

<sup>20</sup>Rutherford Appleton Laboratory, Chilton, Didcot, Oxfordshire, OX11 0QX, UK

<sup>21</sup>DPhPE, CEN Saclay, F-91191 Gif-sur-Yvette, France

<sup>22</sup>Department of Physics, Technion-Israel Institute of Technology, Haifa 32000, Israel

<sup>23</sup>Department of Physics and Astronomy, Tel Aviv University, Tel Aviv 69978, Israel

<sup>24</sup>International Centre for Elementary Particle Physics and Dept of Physics, University of Tokyo, Tokyo 113, and Kobe University, Kobe 657, Japan

# 1 Introduction

There are two principal approaches which are commonly employed when applying perturbative QCD to the description of hadronic final states at high energies. The first is based on a complete order-by-order calculation of Feynman diagrams; in the case of  $e^+e^- \rightarrow$  hadrons the QCD matrix elements are known to  $\mathcal{O}(\alpha_s^2)$ , representing final states of up to four partons. This approach is important, for example, in accurately describing hard gluon emission, but it is inadequate for modelling soft processes, in which multiple gluon emissions have to be considered. In this regime the ‘‘Leading Logarithm Approximation’’ (LLA) [1] is a more appropriate technique, in which the effects of multiple gluon emissions may be calculated, for some processes. A general discussion of the application of QCD at LEP may be found in ref. [2].

One application of the LLA is the calculation of the momentum spectrum of soft gluons. The ‘‘Local Parton-Hadron Duality’’ (LPHD) hypothesis [3] may then be invoked to relate this distribution to the hadron momentum spectrum by a simple normalization factor. These predictions were tested in a previous paper [4] in which the OPAL collaboration presented a measurement of the distribution of  $\xi = \ln(1/x_p)$  for charged particles, where  $x_p = 2p/E_{cm}$ ,  $p$  being the particle momentum and  $E_{cm}$  the centre-of-mass energy. The distribution showed a roughly Gaussian form centred around  $\xi = 3.6$ . Both the shape of the distribution around the peak and its dependence on centre-of-mass energy were well described by analytic QCD calculations in the LLA framework, in which leading and next-to-leading terms were considered. The treatment of coherence effects between soft gluons was important in achieving a good description of the data. Similar results have been found for other particle species at LEP [5].

A recent paper [6] has extended these coherent next-to-leading calculations to the two-particle momentum distribution. In particular the normalized correlation function is calculated:

$$R(\xi_1, \xi_2) = \frac{D^{(2)}(\xi_1, \xi_2)}{D^{(1)}(\xi_1)D^{(1)}(\xi_2)} ;$$

where

$$D^{(1)}(\xi) = \frac{1}{N_{events}} \frac{dn}{d\xi} \quad \text{and} \quad D^{(2)}(\xi_1, \xi_2) = \frac{1}{N_{events}} \frac{d^2n}{d\xi_1 d\xi_2} .$$

$R(\xi_1, \xi_2)$  is symmetric with respect to  $\xi_1$  and  $\xi_2$ . The form of  $R(\xi_1, \xi_2)$  is predicted by QCD, in the next-to-leading logarithm approximation, to be:

$$R(\xi_1, \xi_2) = c_1 + c_2(\xi_1 + \xi_2) + c_3(\xi_1 - \xi_2)^2 , \quad (1)$$

where the coefficients are given in terms of the energy scale  $Q$  (taken to be  $E_{cm}$ ) and a QCD scale parameter  $\Lambda$ :

$$c_1 = 1.375 - \frac{1.262}{(\ln(Q/\Lambda))^{\frac{1}{2}}} , \quad c_2 = \frac{0.877}{(\ln(Q/\Lambda))^{\frac{3}{2}}} , \quad c_3 = -\frac{1.125}{(\ln(Q/\Lambda))^2} . \quad (2)$$

The unknown normalization factor associated with the LPHD hypothesis cancels between  $D^{(1)}$  and  $D^{(2)}$ , and thus the prediction involves just one free parameter, the

effective QCD scale,  $\Lambda$ . The present calculations are not available to sufficiently high order for this to correspond to  $\Lambda_{\overline{MS}}$ , nor is it necessarily the same as the  $\Lambda$  which appears in the analogous calculation of the single-particle spectrum. However, it would be expected to be of comparable magnitude, i.e. a few hundred MeV, and if this were not so it would suggest that higher order contributions are important. The general features predicted are that the correlation should be greatest when the particles have equal momenta ( $\xi_1 = \xi_2$ ) and should increase towards low momentum (large  $\xi$ ). A calculation to leading order [7] predicts a correlation function with the leading asymptotic behaviour of  $c_1$  ( $c_1 = 1.375$ ), and the quadratic coefficient,  $c_3$  (as given in eq.(2)), but no linear term ( $c_2 = 0$ ). The next-to-leading corrections are substantial, and in particular the increase towards large values of  $\xi$  only arises in next-to-leading order.

In this letter we present measurements of  $R(\xi_1, \xi_2)$  for charged particles using the OPAL detector at LEP, and compare them with the analytic QCD predictions. There are no previously published data relating to  $R(\xi_1, \xi_2)$ , so these measurements constitute a new test of QCD. We also compare the data with QCD Monte Carlo calculations. This allows us to investigate the effects of hadronization, and may also provide an interesting new test of the fragmentation models themselves, since the Monte Carlo programs have never been tuned to these features of data.

## 2 The OPAL Detector and Data Sample

A detailed description of the OPAL detector is given in ref. [8]. The detector elements most relevant for this analysis are the central tracking detectors. The central detector components used for the present study were three systems of drift chambers. The innermost is a high precision "vertex detector", of radius 24 cm, providing up to 18 measurements per track with a precision of about 50  $\mu\text{m}$  in the plane transverse to the beams. This is surrounded by a large "jet chamber" which provides up to 159 measured space points per track with a precision of typically 140  $\mu\text{m}$  in the transverse plane. Outside this, at a radius of about 190 cm, is a system of "z-chambers" which allow improved measurement of the polar angle  $\theta$ . These detectors are all located within a solenoidal magnet providing a field of 0.435 T. The momentum resolution may be represented as  $\sigma(p_T)/p_T = \sqrt{(0.0018p_T)^2 + (0.02)^2}$  (with  $p_T$  in GeV/c). The average angular resolution which is currently achieved is about 0.1 mrad in the azimuthal angle about the beam axis and better than 10 mrad in the polar angle.

This analysis is based on charged particles produced in multihadronic decays of the  $Z^0$  boson. The data were collected with the OPAL detector in 1990 and 1991 at centre-of-mass energies between 88.3 and 94.3 GeV. The trigger and multihadronic event selection are discussed in ref. [9] and ref. [10] respectively. Their efficiency for accepting multihadronic events in the angular range used in the present analysis is estimated to be greater than 99.6%. For this analysis, additional criteria were applied in order to eliminate poorly measured tracks and to obtain well contained

events. The central jet chamber and its trigger system were required to be fully operational. Charged tracks were accepted if they originated from within 2 cm of the interaction point in the plane perpendicular to the beams, and within 50 cm in the longitudinal direction. Each charged track was required to have a transverse momentum with respect to the beam direction of more than 150 MeV/c and at least 40 measured space points in the jet chamber. Hadronic events were required to contain at least five charged tracks satisfying the above criteria, the sum of the energies of the charged tracks was required to exceed 5 GeV and the polar angle of the thrust axis was required to satisfy  $|\cos \theta_{thrust}| < 0.9$ . Starting from a data sample of about  $20.8 \text{ pb}^{-1}$ , corresponding to approximately 490,000 multihadronic events collected by OPAL, we obtained 389,195 events after application of these cuts.

### 3 Measurement of $R(\xi_1, \xi_2)$

Using tracks selected by the criteria listed in Sect. 2 we computed the single- and two-particle momentum spectra  $D^{(1)}(\xi)$  and  $D^{(2)}(\xi_1, \xi_2)$  and thus the correlation function  $R(\xi_1, \xi_2)$ . We have concentrated on the region where the  $\xi$  values for both particles satisfied

$$2.5 < \xi < 4.5 \text{ ,}$$

which corresponds to the region in which the analytic QCD calculations gave a satisfactory description of the single-particle spectrum [4]. The particle momenta therefore lie between 0.5 and 3.8 GeV/c. At larger momenta (smaller  $\xi$ ) we would expect contributions from hard processes which may not be correctly reproduced in the LLA QCD calculations, whilst at lower momenta (larger  $\xi$ ) where the momenta become comparable with the pion mass, kinematic effects are likely to become important.

The correlation function was corrected for detector resolution and acceptance effects using a detailed Monte Carlo simulation of the detector [11]. A simple bin-by-bin correction was applied to the correlation, with correction factors given by:

$$C(\xi_1, \xi_2) = \frac{R_{gen}(\xi_1, \xi_2)}{R_{det}(\xi_1, \xi_2)} \text{ ,}$$

where  $R_{gen}$  and  $R_{det}$  refer to the correlation functions of the generated and detected charged particles respectively. The generated charged particles were taken to be those remaining after particles with average lifetimes less than  $3 \times 10^{-10}$  s have decayed. Most acceptance effects cancel in the correlation, with the consequence that the correction factors were very close to unity throughout the momentum range considered; they ranged between 0.997 and 1.014, with an average value of 1.006. For this correction procedure to be valid it is necessary that the bin width be significantly greater than the experimental resolution; this condition is comfortably satisfied by our choice of bins of width  $\Delta\xi = 0.1$ , which compares with the average experimental resolution of  $\delta\xi = 0.023$  in the region under study. The bin width chosen gives

reasonably small statistical errors and is also the same as in our earlier study of the single-particle distribution [4]. The corrections were computed using the JETSET parton shower model [12], with parameters tuned to OPAL data on global event shapes [13], as the input to the detector simulation. A sample of 424,823 Monte Carlo events (after cuts) was used to calculate these corrections.

Systematic uncertainties in the correction factors were assessed by use of a sample of events in which the HERWIG parton shower model [14] was used as the input to the detector simulation program. When these HERWIG events were used to correct the data a small but systematic difference from the data corrected using JETSET was seen, consistent with 0.005 throughout the  $(\xi_1, \xi_2)$  plane. Accordingly a systematic error of  $\pm 0.005$  was assigned to the measured values of  $R(\xi_1, \xi_2)$ .

The event and track selection cuts were varied, and the corrected correlation function was recalculated in each case. In all cases the change in the correlation was completely negligible, and well within the statistical error. As anticipated, systematic uncertainties have a tendency to cancel in the normalized correlation. No additional systematic error was assigned as a result of these studies.

The OPAL detector underwent significant modifications between 1990 and 1991, including the installation of a new beam pipe and a microvertex detector, which led to some differences in the detector acceptance. These effects are adequately modelled by the simulation program, and the corrected data for  $R(\xi_1, \xi_2)$  showed excellent agreement between the two periods, within the statistical errors. We have therefore averaged the two corrected data samples, weighting them by the reciprocals of the squares of the errors.

The corrected correlation function is shown in fig. 1a. The distribution is necessarily symmetric about the line  $\xi_1 = \xi_2$ . We observe that the correlation function is greater than unity in this region of  $(\xi_1, \xi_2)$  space, indicating that positive momentum correlations are present. In order to compare the data with QCD predictions, and in order to present the errors clearly, in the subsequent discussion we show the value of  $R(\xi_1, \xi_2)$  along six narrow bands in the  $(\xi_1, \xi_2)$  plane:

- (I)  $|\xi_1 - \xi_2| < 0.1$
- (II)  $0.4 < \xi_1 - \xi_2 < 0.6$
- (III)  $0.9 < \xi_1 - \xi_2 < 1.1$
- (IV)  $5.9 < \xi_1 + \xi_2 < 6.1$
- (V)  $6.9 < \xi_1 + \xi_2 < 7.1$
- (VI)  $7.9 < \xi_1 + \xi_2 < 8.1$

These bands are shown in fig. 1b, and the values of  $R(\xi_1, \xi_2)$  along these bands are listed in Table 1. The errors include the statistical error on the data and on the correction factors, and also the systematic error  $\pm 0.005$  discussed above, added in quadrature. Bands II, III, V and VI are extended slightly outside the region shown in fig. 1 in order to illustrate the behaviour of the correlation over a wider range.



## 4 Comparison with Analytic QCD calculations

Figure 2 shows the measured data for  $R(\xi_1, \xi_2)$  along the six bands described above. We see that in broad terms the data show the features expected from the QCD formula in eq. (1). These are that the correlation should be strongest when the two particles have the same momentum,  $\xi_1 = \xi_2$ , and that the strength of the correlation should increase towards larger  $\xi$ , i.e. lower momentum. Specifically, the behaviour is predicted to be linear along the lines of constant  $\xi_1 - \xi_2$ , (I, II and III), all with the same slope, and quadratic along the orthogonal lines of constant  $\xi_1 + \xi_2$  (IV, V and VI), all with the same curvature. The data confirm that the correlation is greatest where  $\xi_1 = \xi_2$  (line I) and increases with  $\xi_1 + \xi_2$ . The increase with  $\xi_1 + \xi_2$  demonstrates the importance of the next-to-leading contributions, since the  $c_2$  term in eq. (1) is absent to leading order. However there is evidence for a flattening off of the slope towards large values of  $\xi$ , which is not predicted by the theory.

The curves in fig. 2 show the predictions of eq. (1) for several values of the QCD effective scale  $\Lambda$  in the range 50 MeV to 1 GeV. The value which gave a satisfactory description of the single-particle distribution was  $\Lambda = 255 \pm 26$  MeV [4]. We see that the slopes of the measured correlation in bands I, II, III, and the curvatures along bands IV, V, VI, are broadly similar to those predicted by the analytic QCD formula, but that the theory fails to reproduce the overall level of the correlation in the data for any reasonable value of  $\Lambda$ . This may be demonstrated quantitatively by fitting eq. (1) to the full  $R(\xi_1, \xi_2)$  distribution in the range  $2.5 < \xi < 4.5$ , but treating  $c_1$ ,  $c_2$  and  $c_3$  as independent free parameters. The resulting fit (with  $\chi^2/d.o.f.=1800/207$ ) yielded  $c_1 = 0.928 \pm 0.002$ ,  $c_2 = 0.025 \pm 0.003$  and  $c_3 = -0.021 \pm 0.003$ . If values of  $\Lambda$  are derived from each of these coefficients in turn using eq. (2) we obtain  $32 \pm 2$ ,  $2_{-1}^{+5}$  and  $60_{-27}^{+38}$  MeV respectively. The inconsistency of these values, and the large value of  $\chi^2/d.o.f.$ , indicate that the data cannot be fitted by the present QCD calculations. This suggests that higher order contributions may be important. This may not be unexpected, in view of the dashed curve in fig. 2, which shows the leading order QCD prediction for  $\Lambda = 255$  MeV. This differs substantially from the next-to-leading curve, lying above it over most of the region under consideration. Since the next-to-leading correction is large, it would not be too surprising if still higher order terms were needed. The next order terms are expected to be reduced by an additional factor of  $(\ln(Q/\Lambda))^{-\frac{1}{2}}$  with respect to those in eq.(2) [15], and terms of this form with coefficients of order unity could account for the discrepancies between the fitted and calculated  $c$  values.

## 5 Comparison with QCD Monte Carlo programs

Having seen that the analytic QCD calculations are unable to account for the data, it is instructive to examine QCD Monte Carlo models, which in some sense incorporate higher order effects through the hadronization process. We discuss the following models:

- JETSET version 7.3 [12] with a coherent parton shower and string fragmentation. The parameters were tuned to fit OPAL data on event shapes [13]. The JETSET model offers many convenient mechanisms for changing the parton shower and hadronization parameters, some of which we discuss below.
- HERWIG version 5.4 [14] with a coherent parton shower and cluster fragmentation. The parameters were tuned to fit OPAL data on event shapes<sup>1</sup>.
- ARIADNE version 3.1 [16] with a coherent parton shower based on a colour dipole formulation and string fragmentation. The parameters were tuned to fit OPAL data on event shapes [13].
- COJETS version 6.12 [17] with an incoherent parton shower and independent fragmentation. The parameters were tuned by the authors to fit OPAL data on event shapes. We also examined COJETS version 6.20, which uses different fragmentation parameters for quarks and gluons in an attempt to fit data on the “string effect” at LEP [18].

In fig. 3 we compare our data with the three coherent parton shower models, JETSET, HERWIG and ARIADNE. ARIADNE gives an excellent fit to the data throughout. JETSET lies slightly below the data (by 0.010 on average), while HERWIG is the least successful of these models, showing stronger correlations than the data (by 0.024 on average), and particularly overestimating the correlations at large values of  $\xi$ . It should be recalled that the parameters of the Monte Carlo models were chosen by fitting data on global event shapes, and that this fitting procedure therefore led to estimates of the uncertainties on these parameters. We have investigated the effect of varying the string hadronization parameters  $a$  and  $\sigma_q$  of JETSET within the ranges given in ref. [13], and find that the values of  $R(\xi_1, \xi_2)$  vary by about  $\pm 0.006$  on average. These variations are thus comparable with the size of the differences between the data and the JETSET model. If the parameters of HERWIG are similarly altered we find that  $R(\xi_1, \xi_2)$  varies over a range of about  $\pm 0.007$ . We thus conclude that the data do not show any substantial disagreement with these models when reasonable uncertainties in the hadronization parameters (such that the global event shapes are still well modelled) are taken into account, with the possible exception of HERWIG in the large  $\xi$  region.

In fig. 4 we compare our data with incoherent parton shower models. Neither of the versions of COJETS gives a particularly good representation of the correlation data, with version 6.12 tending to underestimate the correlation, and version 6.20 yielding too strong a correlation especially at large  $\xi$  (low momentum). However, in the latter case the agreement is at least as good as with HERWIG (fig. 3). We have also taken JETSET, with coherence effects disabled, and reoptimized the string hadronization parameters so as to fit the OPAL event shape data as well as the

---

<sup>1</sup>The tuning procedure follows ref. [13], though HERWIG 5.4 includes the exact first order QCD matrix element, which leads to a much better fit to the event shape data than HERWIG 3.4 which was considered in ref. [13]. With version 5.4 the fit is essentially as good as with JETSET. The OPAL-tuned parameters are the defaults in HERWIG 5.4.

single-particle distribution<sup>2</sup>. We see that this version of the model yields a result very similar to version 6.20 of COJETS. If instead we use the independent fragmentation option in JETSET with coherence disabled (not shown) the agreement with data is significantly less good, with an even stronger correlation at large  $\xi$ . In this context it may be useful to recall our analysis of the single-particle distribution [4], where it was found that an incoherent model, based on JETSET, could fit the data if string fragmentation were employed, but not if independent fragmentation was chosen.

We have used the JETSET model to investigate other non-perturbative effects which could be expected to affect the correlations. In most cases the effects prove to be small, and certainly insufficient to explain the large difference in the level of the correlations between the analytic calculations and the data. We therefore describe the results of these studies briefly, without showing detailed results in figures.

Our standard version of JETSET does not include the effect of Bose-Einstein correlations between mesons, although these have been observed in data at LEP [19, 20]. Bose-Einstein correlations may, however, be implemented in the model as an option. When this was done, the two-particle correlation in the model was slightly increased along band I ( $\xi_1 = \xi_2$ ) only, particularly at high  $\xi$  or low momentum, and in fact gave better agreement with the data. In the region  $7 < \xi_1 + \xi_2 < 9$  along band I  $R(\xi_1, \xi_2)$  rose by 0.016 on average.

The presence of resonance decays might also be expected to influence the level of correlation. We have pursued two approaches to assess the influence of resonance decays. Firstly, we reduced by a factor of two the production of vector mesons in JETSET, adjusting the other hadronization parameters so as to maintain a good description of the event shape and single-particle data, but not modifying the parameters governing the parton shower<sup>3</sup>. These changes in the model caused a negligible change in the correlations. Secondly, we examined the correlations between the charged hadrons in JETSET at the stage before resonance decays (of the  $1^-$  light meson nonet, the  $\frac{3}{2}^+$  light baryon decuplet and the  $\eta$  and  $\eta'$  mesons) and weak decays of strange mesons and baryons were performed. One might hope that these “primary” hadrons would reflect the underlying soft parton structure more closely. We found that the value of  $R(\xi_1, \xi_2)$  was slightly increased at lower values of  $\xi$ , and reduced at large values, so that the slope along bands I, II and III was much reduced. The overall level was scarcely affected, so that agreement with the analytic QCD calculations was in no way improved. We also considered the effect of including all final state particles, both charged and neutral, instead of just charged particles in the correlation – this led to a small systematic reduction of the correlation by 0.014.

As a further investigation of the effects of hadronization, we have examined JETSET with the QCD  $\mathcal{O}(\alpha_s^2)$  matrix element option and string fragmentation,

---

<sup>2</sup>The parameters used were: MSTJ(42) = 1, MSTJ(44) = 1, PARJ(81) =  $\Lambda$  = 0.44 GeV, PARJ(82) =  $Q_0$  = 1.45 GeV, PARJ(21) =  $\sigma_q$  = 0.44 GeV, PARJ(41) =  $a$  = 0.18 and PARJ(42) =  $b$  = 0.65 GeV<sup>2</sup>.

<sup>3</sup>Those parameters modified from our default values were: PARJ(11) = 0.25, PARJ(12) = 0.30, PARJ(13) = 0.375 to reduce the vector meson yield, and PARJ(21) =  $\sigma_q$  = 0.33 GeV, PARJ(41) =  $a$  = 0.34 to achieve the correct multiplicity and event shapes.

with parameters tuned to OPAL data as described in ref. [21]. This model includes only a small part of the gluon coherence effects, from the  $q\bar{q}gg$  final state, so in the region we are studying we may expect most of the correlation to come from the string hadronization. Although this model fits the OPAL event shape data significantly less well than the parton shower models, it nevertheless gives a reasonably good description of the correlations, especially for  $\xi_1 + \xi_2 < 7$ , though it flattens off and slightly underestimates the correlation at larger  $\xi$ . For example, in the region  $5 < \xi_1 + \xi_2 < 7$  along band I  $R(\xi_1, \xi_2)$  lay below the data by 0.010 on average, whilst in  $7 < \xi_1 + \xi_2 < 9$  the average discrepancy was 0.021.

## 6 Discussion and Summary

We have presented, for the first time, data on two-particle momentum correlations at small momentum fractions in hadronic final states produced in  $e^+e^-$  collisions. The data have been compared with QCD calculations performed in the (next-to-) leading logarithm approximation, which are closely related to calculations which were successfully applied to the description of single-particle spectra at LEP and in  $e^+e^-$  experiments at lower energies. The data exhibit a positive correlation, with the general features predicted by the analytic QCD calculations, namely a correlation which is greatest when the particles have equal momenta, and which increases towards low momenta. However, the overall level of the correlation lies significantly below the QCD prediction, for any reasonable value of the QCD effective scale parameter  $\Lambda$ . It therefore appears that higher order corrections may not be negligible, and/or that hadronization effects are likely to be significant given the presently available QCD calculations. Indeed, the next-to-leading contribution in eq.(2) is sizeable, so it would not be surprising if higher orders still were needed in order to describe the data. It should also be noted that the prediction for the single-particle distribution contains an arbitrary normalization factor, which might be able to absorb some of the higher order effects in the single-particle case, but which cancels in the definition of the two-particle correlation.

This situation is reminiscent of the behaviour which has been seen for the higher moments of the charged multiplicity distribution for  $e^+e^- \rightarrow$  hadrons. The multiplicity moments  $\langle n \rangle$  and  $\langle n(n-1) \rangle$  are simply the integrals over  $\xi$  of the momentum spectra  $D^{(1)}$  and  $D^{(2)}$  which contribute to the correlation  $R(\xi_1, \xi_2)$ . The next-to-leading QCD prediction for the average multiplicity  $\langle n \rangle$  is known, up to a normalization constant, and the data can be well fitted by the QCD form with a reasonable value of  $\Lambda$ , around 140 MeV [22, 23, 24]. The QCD prediction for the second binomial moment  $\langle n(n-1) \rangle$  is also available, and if the ratio  $\frac{\langle n(n-1) \rangle}{\langle n \rangle^2}$  is formed the normalization cancels and the prediction depends on the QCD scale  $\Lambda$  only. The next-to-leading term in the QCD calculation of  $\frac{\langle n(n-1) \rangle}{\langle n \rangle^2}$  is however quite large, and the data cannot be described with a reasonable value of  $\Lambda$  [23], the QCD prediction lying above the data, indicating the importance of yet higher orders.

Comparison between the data and parton shower Monte Carlo models based on

the LLA approach shows good agreement in general. ARIADNE gives the closest agreement with the data. JETSET slightly underestimates the level of correlation, but is probably not incompatible once systematic uncertainties are taken into account. HERWIG predicts too strong a correlation, especially at low momentum. The results seem not to be too sensitive to the presence of coherence in the parton shower, so long as the hadronization parameters are appropriately tuned to fit other features of the data. Likewise, a model based on the  $\mathcal{O}(\alpha_s^2)$  matrix element formulation of QCD with string fragmentation, which embodies rather little explicit coherence, also fits the data quite well. The effect of Bose-Einstein correlations on the two-particle correlation appears to be rather small, and is only evident where  $\xi_1$  and  $\xi_2$  are nearly equal and both large (i.e. at low momentum). The effect of resonance decays on the overall level of the correlation function also seems to be rather small, and principally affects the lower  $\xi$  region. Thus uncertainties in resonance yields are unlikely to influence our results.

It may be noted that the QCD Monte Carlo models generally differ from one another much more at the parton level than at the hadron level. In no case does the correlation at the parton level agree with the correlation predicted in eqs.(1) and (2). There are differences in the way the leading log approximation is implemented in different models [25]. Furthermore, there are differences in the treatment of mass effects and cutoffs in the Monte Carlo models compared to the analytical calculations. One effect is that the momentum distributions of the partons in the Monte Carlo models cut off within the region of  $\xi$  considered for the present analysis, so that it is not appropriate to compare the two-particle correlation for the partons in the models with the analytic QCD calculations.

In summary, we have presented new data on two-particle momentum correlations, for comparison with recent analytic QCD calculations. Since there is no arbitrary normalization factor in the analytic calculation, the two-particle correlations could be regarded as a more stringent test of the QCD calculations than the analogous single-particle distribution which has hitherto been investigated. The observed correlation exhibits the general features predicted, though with some significant differences, which may plausibly be attributed to terms of higher order than presently calculated. QCD Monte Carlo models, despite substantial differences in their treatment at the parton level, are seen to describe the data at the hadron level quite well. This suggests that, given the order to which the analytic QCD calculations are currently available, the correlation may be significantly modified by hadronization effects, which could presumably absorb the higher order effects, or equivalently that the LPHD hypothesis may not be applicable in this case. It therefore seems likely that higher order calculations would be needed in order to achieve anything more than qualitative agreement between analytic QCD predictions and data for two-particle correlations.

## 7 Acknowledgements

We thank B.R. Webber and C.P. Fong for illuminating discussions.

We also thank the SL Division for the efficient operation of the LEP accelerator and their continuing close cooperation with our experimental group. In addition to the support staff at our own institutions we are pleased to acknowledge the

Department of Energy, USA,

National Science Foundation, USA,

Science and Engineering Research Council, UK,

Natural Sciences and Engineering Research Council, Canada,

Israeli Ministry of Science,

Minerva Gesellschaft,

Japanese Ministry of Education, Science and Culture (the Monbusho) and a grant under the Monbusho International Science Research Program,

American Israeli Bi-national Science Foundation,

Direction des Sciences de la Matière du Commissariat à l'Energie Atomique, France,

Bundesministerium für Forschung und Technologie, FRG,

National Research Council of Canada, Canada,

A.P. Sloan Foundation and Junta Nacional de Investigação Científica e Tecnológica, Portugal.

## References

- [1] Yu.L. Dokshitzer, V.A. Khoze, A.H. Mueller and S.I. Troyan, "Basics of Perturbative QCD", Editions Frontières (1991).
- [2] Z. Kunszt, P. Nason, G. Marchesini and B.R. Webber, "QCD" in "Z Physics at LEP 1", CERN 89-08, vol. 1, eds. G. Altarelli, R. Kleiss and C. Verzegnassi (Geneva 1989).
- [3] D. Amati and G. Veneziano, Phys. Lett. **B83** (1979) 87;  
Ya.I. Azimov, Yu.L. Dokshitzer, V.A. Khoze and S.I. Troyan, Z. Phys. **C27** (1985) 65
- [4] OPAL Collab., M.Z. Akrawy et al., Phys. Lett. **B247** (1990) 617.
- [5] L3 Collab., B. Adeva et al. Phys. Lett. **B259** (1991) 199;  
OPAL Collab., G. Alexander et al., Phys. Lett. **B264**(1991) 467;  
DELPHI Collab., P. Abreu et al., Phys. Lett. **B275**(1992) 231.
- [6] C.P. Fong and B.R. Webber, Nucl. Phys. **B355** (1991) 54;  
C.P. Fong, Ph.D. Thesis, University of Cambridge (October 1991).
- [7] Yu.L. Dokshitzer, V.S. Fadin and V.A. Khoze, Z. Phys. **C18** (1983) 37.
- [8] OPAL Collab., K. Ahmet et al., Nucl. Instrum. Methods **A305** (1991) 275.
- [9] M. Arignon et al., Nucl. Instrum. Methods **A313** (1992) 103.
- [10] OPAL Collab., G. Alexander et al., Z. Phys. **C52** (1991) 175.
- [11] J. Allison et al., Comput. Phys. Commun. **47** (1987) 55;  
D.R. Ward, Proc. MC'91 Workshop, NIKHEF, Amsterdam (1991) 204;  
J. Allison et al., CERN-PPE/91-234, to be published in Nucl. Instrum. Methods.
- [12] T. Sjöstrand, Comput. Phys. Commun. **39** (1986) 347;  
T. Sjöstrand and M. Bengtsson, Comput. Phys. Commun. **43** (1987) 367.
- [13] OPAL Collab., M.Z. Akrawy et al., Z. Phys. **C47** (1990) 505.
- [14] G. Marchesini and B.R. Webber, Nucl. Phys. **B310** (1988) 461;  
G. Marchesini et al., Comput. Phys. Commun. **67** (1992) 465.
- [15] B.R. Webber, private communication.
- [16] U. Pettersson, LU TP 88-5 (1988);  
L. Lönnblad and U. Pettersson, LU TP 88-15 (1988);  
L. Lönnblad, LU TP 89-10 (1988).
- [17] R. Odorico, Comput. Phys. Commun. **32** (1984) 139;  
R. Odorico, Comput. Phys. Commun. **59** (1990) 527.  
P. Mazzanti and R. Odorico, Nucl. Phys. **B370** (1992) 23.

- [18] OPAL Collab., M.Z. Akrawy et al., Phys. Lett. **B261** (1991) 334.
- [19] OPAL Collab., P.D. Acton et al., Phys. Lett. **B267** (1991) 143.
- [20] ALEPH Collab., D. Decamp et al., Z. Phys. **C54** (1992) 75.
- [21] OPAL Collab., P.D. Acton et al., Phys. Lett. **B276** (1992) 547.
- [22] DELPHI Collab., P. Abreu et al., Z. Phys. **C50** (1991) 185.
- [23] ALEPH Collab., D. Decamp et al., Phys. Lett. **B273** (1991) 181.
- [24] OPAL Collab., P.D. Acton et al., Z. Phys. **C53** (1992) 539.
- [25] T. Sjöstrand et al., "QCD Generators" in "Z Physics at LEP 1", CERN 89-08, vol. 3, eds. G. Altarelli, R. Kleiss and C. Verzegnassi (Geneva 1989).



	Band I ( $ \xi_1 - \xi_2  < 0.1$ )	Band II ( $0.4 < \xi_1 - \xi_2 < 0.6$ )	Band III ( $0.9 < \xi_1 - \xi_2 < 1.1$ )
$\xi_1 + \xi_2$	$R(\xi_1, \xi_2)$	$R(\xi_1, \xi_2)$	$R(\xi_1, \xi_2)$
5.1	$1.046 \pm 0.007$	$1.016 \pm 0.006$	$0.990 \pm 0.006$
5.3	$1.057 \pm 0.007$	$1.034 \pm 0.006$	$1.001 \pm 0.006$
5.5	$1.049 \pm 0.007$	$1.041 \pm 0.006$	$1.012 \pm 0.006$
5.7	$1.066 \pm 0.007$	$1.053 \pm 0.006$	$1.028 \pm 0.006$
5.9	$1.077 \pm 0.007$	$1.064 \pm 0.006$	$1.037 \pm 0.006$
6.1	$1.082 \pm 0.007$	$1.070 \pm 0.006$	$1.052 \pm 0.006$
6.3	$1.094 \pm 0.007$	$1.078 \pm 0.006$	$1.057 \pm 0.006$
6.5	$1.102 \pm 0.007$	$1.090 \pm 0.006$	$1.067 \pm 0.006$
6.7	$1.117 \pm 0.007$	$1.095 \pm 0.006$	$1.075 \pm 0.006$
6.9	$1.116 \pm 0.007$	$1.104 \pm 0.006$	$1.082 \pm 0.006$
7.1	$1.122 \pm 0.007$	$1.108 \pm 0.006$	$1.082 \pm 0.006$
7.3	$1.126 \pm 0.007$	$1.112 \pm 0.006$	$1.088 \pm 0.006$
7.5	$1.133 \pm 0.007$	$1.121 \pm 0.006$	$1.099 \pm 0.006$
7.7	$1.123 \pm 0.007$	$1.117 \pm 0.006$	$1.096 \pm 0.006$
7.9	$1.133 \pm 0.007$	$1.116 \pm 0.006$	$1.100 \pm 0.006$
8.1	$1.125 \pm 0.006$	$1.116 \pm 0.006$	$1.104 \pm 0.006$
8.3	$1.137 \pm 0.006$	$1.120 \pm 0.006$	$1.103 \pm 0.006$
8.5	$1.130 \pm 0.006$	$1.120 \pm 0.006$	$1.107 \pm 0.006$
8.7	$1.126 \pm 0.006$	$1.128 \pm 0.006$	$1.113 \pm 0.006$
8.9	$1.141 \pm 0.006$	$1.133 \pm 0.006$	$1.122 \pm 0.006$
	Band IV ( $5.9 < \xi_1 + \xi_2 < 6.1$ )	Band V ( $6.9 < \xi_1 + \xi_2 < 7.1$ )	Band VI ( $7.9 < \xi_1 + \xi_2 < 8.1$ )
$ \xi_1 - \xi_2 $	$R(\xi_1, \xi_2)$	$R(\xi_1, \xi_2)$	$R(\xi_1, \xi_2)$
0.1	$1.080 \pm 0.006$	$1.119 \pm 0.006$	$1.128 \pm 0.006$
0.3	$1.079 \pm 0.006$	$1.112 \pm 0.006$	$1.129 \pm 0.006$
0.5	$1.069 \pm 0.006$	$1.108 \pm 0.006$	$1.116 \pm 0.006$
0.7	$1.062 \pm 0.006$	$1.098 \pm 0.006$	$1.111 \pm 0.006$
0.9	$1.047 \pm 0.006$	$1.097 \pm 0.006$	$1.109 \pm 0.006$
1.1	$1.038 \pm 0.006$	$1.084 \pm 0.006$	$1.098 \pm 0.006$
1.3	$1.030 \pm 0.006$	$1.071 \pm 0.006$	$1.096 \pm 0.006$
1.5	$1.011 \pm 0.006$	$1.062 \pm 0.006$	$1.084 \pm 0.006$
1.7	$1.004 \pm 0.006$	$1.048 \pm 0.006$	$1.080 \pm 0.006$
1.9	$0.985 \pm 0.006$	$1.040 \pm 0.006$	$1.072 \pm 0.006$

Table 1: Measured values of the two-particle correlation  $R(\xi_1, \xi_2)$ . The values in the leftmost column refer to the centres of the bins, which are of width  $\pm 0.1$ . The data are corrected for the finite acceptance and resolution of the detector. The errors include statistical and systematic uncertainties, added in quadrature.

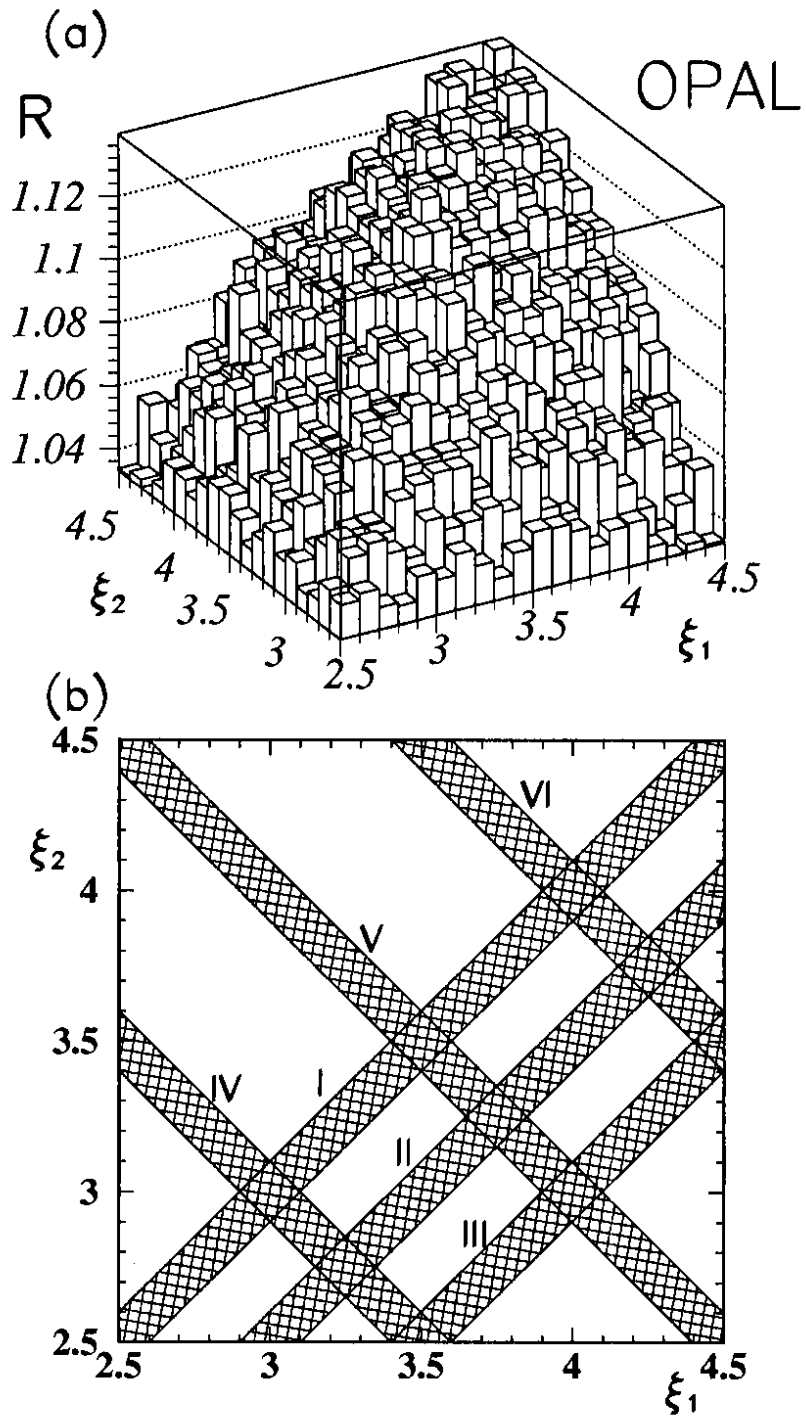


Figure 1: (a) The two-particle momentum correlation function  $R(\xi_1, \xi_2)$  plotted as a function of  $\xi_1$  and  $\xi_2$  (b) bands in the  $(\xi_1, \xi_2)$  plane along which the values of the correlation will be plotted.

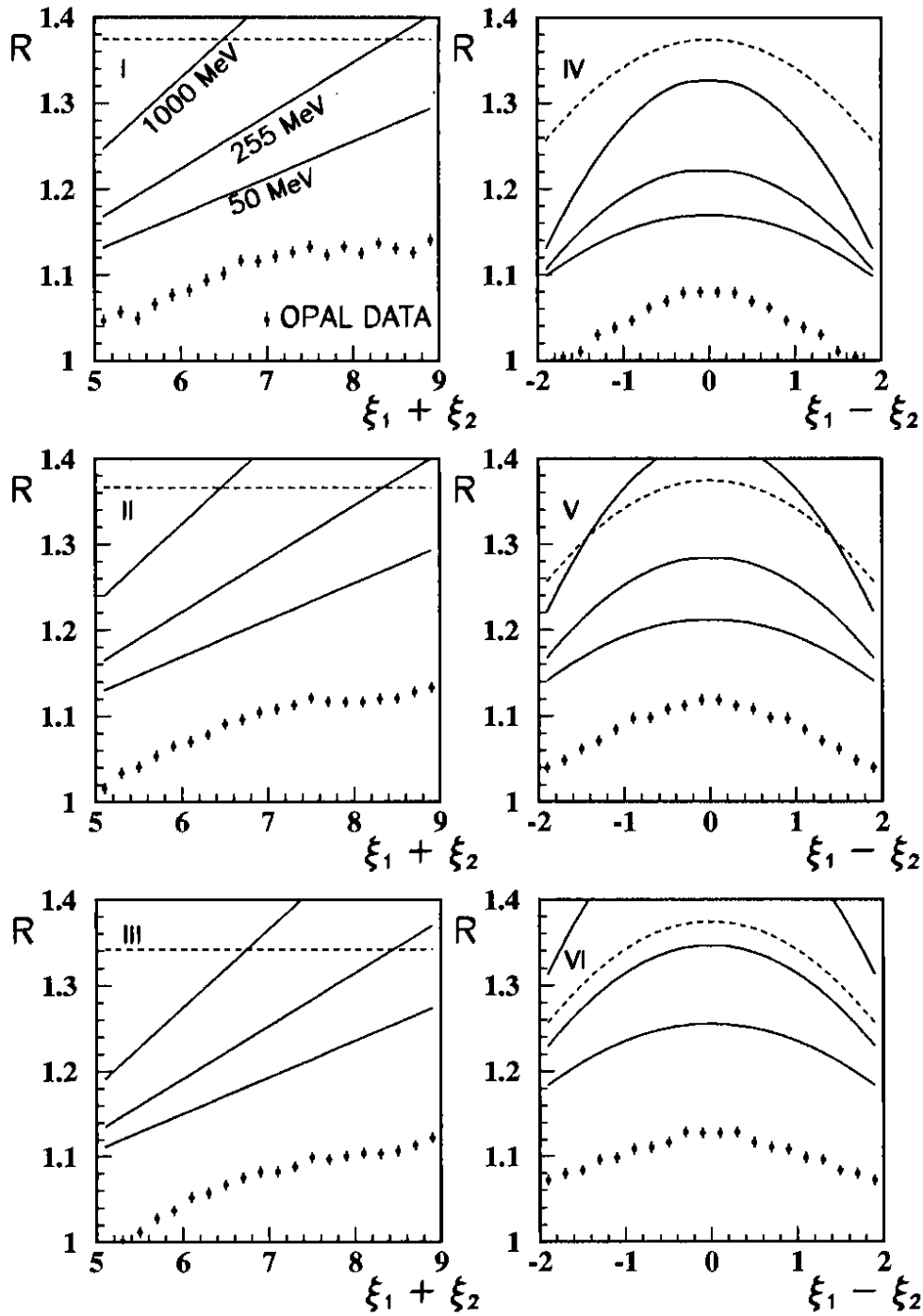


Figure 2: Comparison of data with analytic QCD calculations. Note that the zero is suppressed on the  $R$  axis. The three solid curves represent the next-to-leading QCD calculations for three values of  $\Lambda$ , 1000 MeV (highest curve), 255 MeV (the value which best described the single-particle data) and 50 MeV (lowest curve). The dashed curves indicate the leading order QCD calculations for  $\Lambda = 255$  MeV.

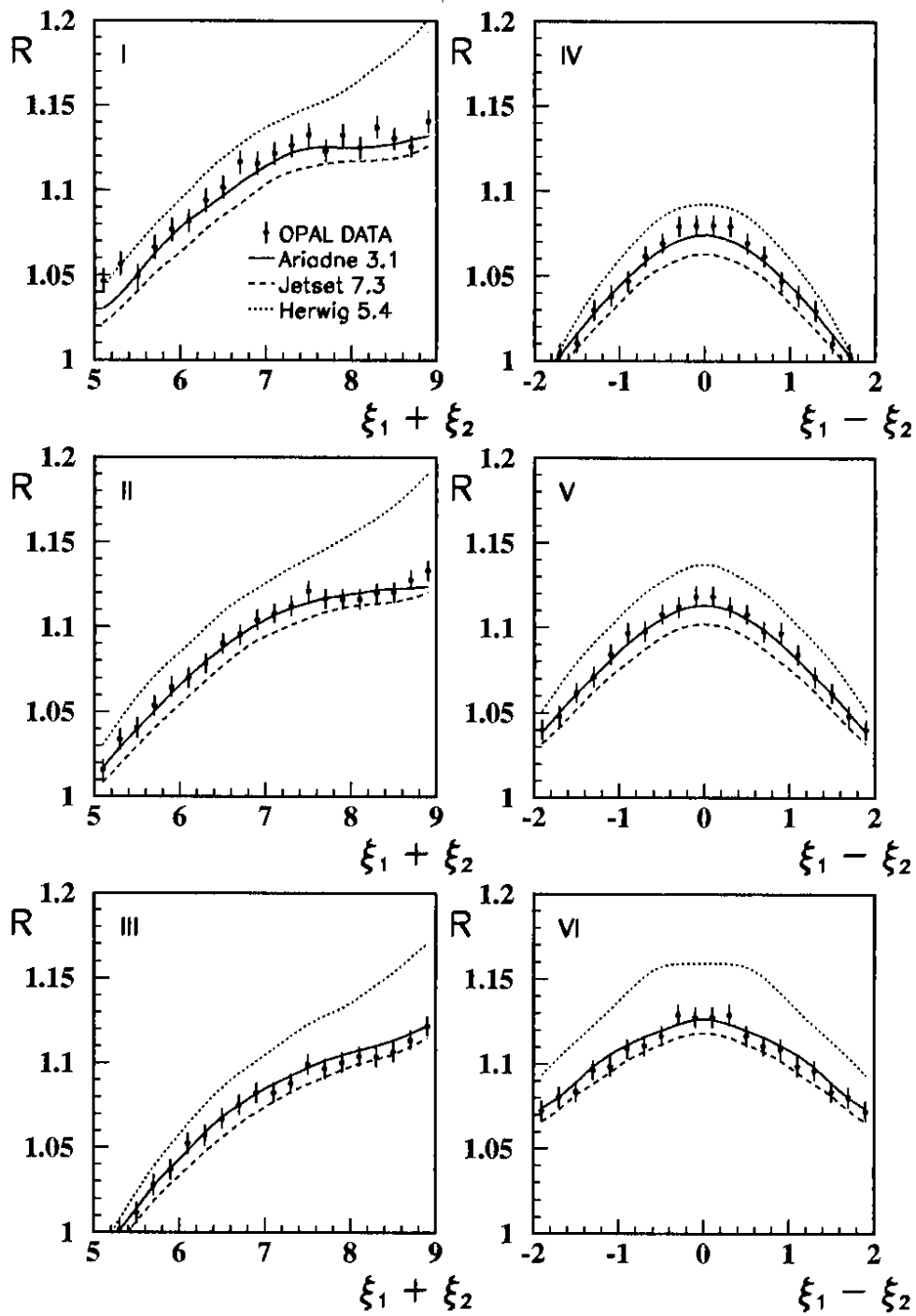


Figure 3: Comparison of data with coherent parton shower Monte Carlo models, ARIADNE (solid), JETSET (dashed) and HERWIG (dotted).

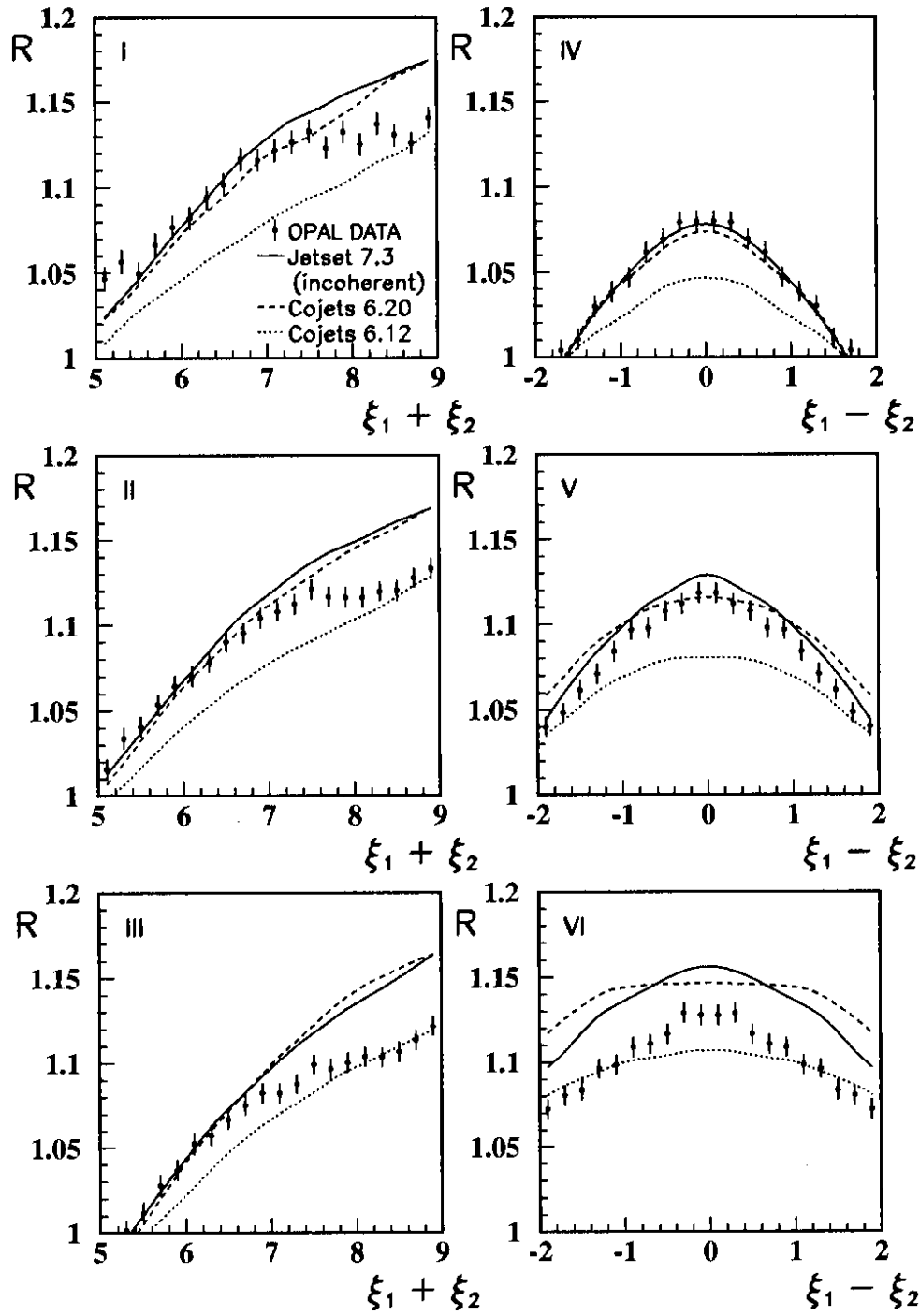


Figure 4: Comparison of data with incoherent parton shower Monte Carlo models, JETSET (solid) and two versions of COJETS (dashed and dotted).